CHEMICAL ENGINEERING TRANSACTIONS, Volume 16, 2008
Guest Editor Eliseo Ranzi
 ISBN 978-88-95608-03-7 ISSN 1974-9791

Characterization of Particles formed in Methane and Ethylene Opposed-flow Diffusion Flames

Mario Commodo, Mariano Sirignano, Andrea D'Anna
Dipartimento di Ingegneria Chimica – Università "Federico II", P.le V. Tecchio, 80 – 80125 – Naples - ITALY

Rocco Pagliara, Patrizia Minutolo
Istituto di Ricerche sulla Combustione – CNR, P.le V. Tecchio, 80 – 80125 – Naples - ITALY

In the this work an experimental and numerical study on particles formation in opposed-flow diffusion flames, burning methane and ethylene as fuel is presented. Spectrally resolved laser induced emission spectroscopy techniques in the ultraviolet and visible, such as fluorescence and incandescence , are here used in order to investigate particles inception and growth with high spatial resolution and in a wide range of flame conditions. The fourth harmonic of a Nd:YAG laser, 266 nm, is used with the purpose to follow combustion generated compounds and their dynamics in flame. A complete kinetic scheme, which provides both to gas-phase and particle reactions, is adopted for numerical simulation. The comparison between experimental results and numerical predictions gives a qualitative view of the mechanism of particle formation.
Both the experimental and numerical results carried out in this work demonstrate and explain the sensibility of inception and growth of soot to radicals concentrations and temperature conditions.

1. Introduction

Combustion-generated particles have gained significant interest because of their direct health and environmental effects (Dockery et al. 1993). In recent years, researchers have focused their attention on ultrafine particles with sizes down to a few nanometers, the most likely to cause the observed effects (Oberdorster et al. 2002). Ultrafine particles formed in combustion systems show mainly a bimodal size distribution function with a first mode peaked at about 1-3nm and a second mode constituted of particles with mean sizes of 10-20nm (D'Alessio et al. 1998, Sgro et al. 2003, Zhao et al. 2003). However, many of these scientific works are carried out on laminar premixed flames for their easier fluidodynamic configurations and modelling interpretation, whereas real combustion conditions are more similar to diffusion controlled ones.
Therefore, following the need to describe particles inception and growth in diffusion controlled systems with high spatial resolution, an opposed-flow configuration has been chosen in the present work in order to study behaviour and sooting tendency of fuels, avoiding fluidodynamic problems fundable in co-flow diffusion flames laminar or turbulent. On the other hand, for co-flow flames, the study of particles inception and growth is much more complex than for the opposed-flow system since they are

Please cite this article as: Commodo M., Siringano M., D'Anna A., Pagliara R. and Minutolo P., (2008), Characterization of particles formed in methane and ethylene opposed-flow diffusion flames, Chemical Engineering Transactions, 16, 259-266

intrinsically two dimensional compared to a quasi-one dimensional opposed-flow (Hwang and Chung 2001). Moreover, soot formation in opposed-flow diffusion flames has been extensively investigated because of its relevance to turbulent flames in the laminar flamelet model.

In the present work, two different fuels: ethylene and methane, in comparable conditions, have been investigated, experimentally and by numerical simulation.

The experimental detection of combustion-byproducts is attempted by UV laser induced emission spectroscopy. The fourth harmonic of a pulsed Nd:YAG laser (266 nm) is used, in order to enhance fluorescence from molecular particles within the flame and also to allow larger soot particles to heat up and emit incandescent radiation (Vander Wal 1996).

Modeling of particles concentration is performed by using a detailed gas-phase chemical kinetics coupled with aerosol dynamic equations using a discrete size spectrum (D'Anna et al. 2005, 2007, 2008).

The Comparison of model results with laser induced emission signals, is proposed, in order to contribute to the understanding of the process of particle inception and dynamic in diffusion controlled conditions.

2. Experimental set-up

The opposed-flow burner system was the same as that of Olten and Senkan (1999). The ethylene and methane diffusion flames were stabilized between two opposed jet nozzles (ID 2.54 cm). The oxidizer stream containing a mix of O2 and Ar was introduced from the upper nozzle; the fuel stream was introduced from the lower nozzle. All gases used were of high purity. Screens were used at the exit of each jet to establish uniform gas flow velocities and to generate stable, flat flames. Nitrogen was used to shield and protect the flame from the surrounding air. The oxidizer and fuel stream velocities were fixed at 16.1 and 13.2 cm/s, respectively. The distance between the two burners was maintained at 1.5 cm for both flames. The global strain rate was maintained constant at 37.7 s-1 for the two flames. Percentage of hydrocarbon, respectively methane and ethylene, in fuel stream was fixed at 75% in Argon, whereas the oxidizer streams consisted of 20% by volume O_2 and the remaining Argon.

In the chosen experimental conditions the flame front and the soot formation zone are located on the oxidizer side. Particles are hence transported away from the flame toward the fuel side. In this way, soot oxidation is absent and the flame is classified "soot forming" (SF) (Hwang and Chung 2001).

The stagnation plane was estimated by seeding the fuel stream with 1 μm-TiO2 particles and measuring the scattering coefficient along the flame axis. TiO2 particles give a strong scattering signal in the fuel side which vanishes at the stagnation point where particles are convected away. Spectrally resolved, laser induced emission measurements were performed by using the fourth harmonic (λ_0=266nm) of a pulsed Nd-YAG laser as exciting source. The energy of the laser pulse was kept constant at 1.5mJ with a pulse duration of 8ns. The light emission was focused onto the 280 nm entrance slit of a spectrometer and detected by a gated ICCD camera . Emission spectra, averaged over 150 scans, were recorded by using an acquisition duration of 20 ns synchronized with the laser pulse. A correction was applied for the wavelength-dependent sensitivity of the

camera. Calibration of laser induced emission signals (LIF and LII) was made by measuring the scattering signal for cold ethylene.

3. Flame modelling

The kinetic scheme of D'Anna (2001, 2005), is used for the modeling of the flame structure and particulate formation. The kinetic scheme includes growth of species by fuel pyrolysis, particulate formation, growth, aggregation and oxidation. PAH formation includes reaction pathways leading to the formation of nanometric-sized particles and their coagulation to larger soot particles. A discrete-sectional approach, D'Anna, Kent 2006, is used for the gas-to-particle process; the ensemble of compounds with molecular mass higher than the largest aromatic compound in the gas-phase is divided into classes of different molecular mass and all reactions are treated in the manner of gas phase chemistry using compound properties such as mass and the numbers of carbon and hydrogen atoms averaged within each section. Particle size distributions are obtained by solution of the transport equation for each section. A brief summary of the scheme is given here. Cunningham's theory is considered to calculate diffusivity of particles. Thermophoretic effect, strongly enhanced in opposed-flow configuration, is taken in account for all sections (Wang 2004).

4. Results and Discussion

Typical emission spectra for the ethylene flame are reported in Fig.1. It shows the different laser induced emission spectra taken at different flame location: starting from the fuel side the spectrum shows a broad fluorescence signal peaked at about 330 nm, across the stagnation plane the spectra shows a fluorescence with a maximum at 430 nm and a continuum which extends into the visible that is attributable to incandescence of soot particles; in the oxidizer side, close to the maximum flame temperature the emission spectrum shows a fluorescence peaked at 300 nm. Moreover in all location it is observable a strong scattering signal at 266 nm.

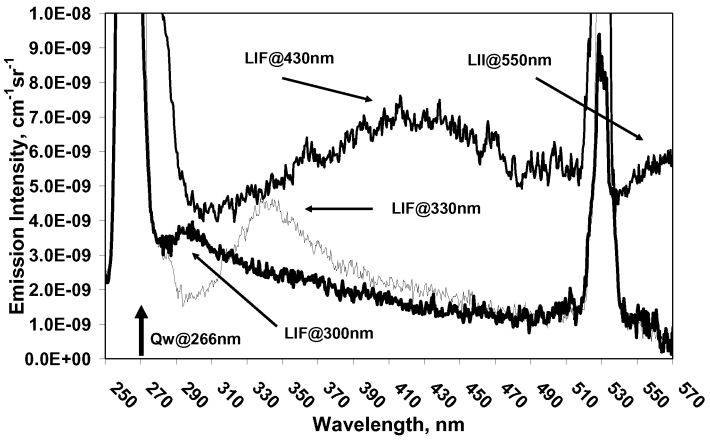

Fig. 1 Emission spectra measured in the ethylene opposed-flow flame in different flame zone.

The different laser induced emission signals can be correlated to different classes of combustion-formed compounds.
Usually fluorescence at 300 nm is correlated to benzene and derivatives whereas higher molecular mass compounds are linked to higher wavelength. LII is generally used to detect soot, because of its spectroscopic behaviour radiation (Vander Wal 1996, 1997).
Modeling helps to localize both maximum of temperature and stagnation plane for all flames.
Moreover predictions of particle concentration and size allows to compare different wavelength signals to different particle classes. Indeed, the use of the sectional method allows to obtained numerically the molecular mass distribution of combustion-formed species with molecular masses higher than the gas-phase PAHs.
Figure 2 reports a typical molecular weight distribution predicted by the model. Four fundamental types of particles by molecular mass can be distinguished: high-molecular mass PAHs with masses between 300 and 1000u, (particles with equivalent sizes of about 1nm), molecular particles with masses between 1000 and 10,000u (particles with equivalent sizes from 1 to 3 nm), nanoparticles with masses between 10,000 and 100,000u (particles with equivalent sizes from 3 to 6 nm) and primary soot particles with masses higher than 100,000u (particles with equivalent sizes larger than 6).

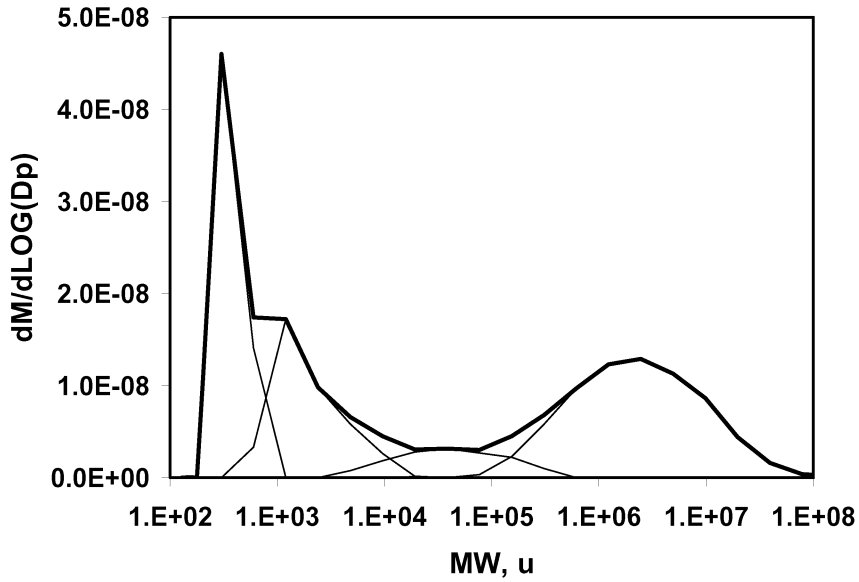

Fig. 2 *Predicted molecular weight distribution function (heavy line). Light lines represent the contribution of four fundamental classes of particles.*

The four peaks in the molecular weight distribution reflect the sequential formation of these species: the first peak is due to PAHs formed in gas-phase by the mechanism of acetylene addiction to aromatic radicals, whereas the last two are due to coagulation of molecular particles which evolves in two peaks due to the size-dependent coagulation rate used.

Comparison between the measured signals of fluorescence and incandescence at different wavelengths and different particle classes concentration, obtained by numerical simulation, are reported in Fig. 3 for methane and in Fig. 4 for ethylene.
The four classes of particles have been determined according to the molecular weight distribuition and divided in high-molecular mass PAHs (HMM-PAH), molecular particles (1nm<Dp<3nm), nanoparticles (3nm<Dp<6nm) and primary soot particles (Dp>6nm).
Their concentration profiles are compared with the four laser induced emission signals: LIF@300nm, LIF@330nm, LIF@440nm and LII@550nm multiplied by four different scale factors respectively.
There is a good correlation between the four different classes of particles and the emission signals for both flames.

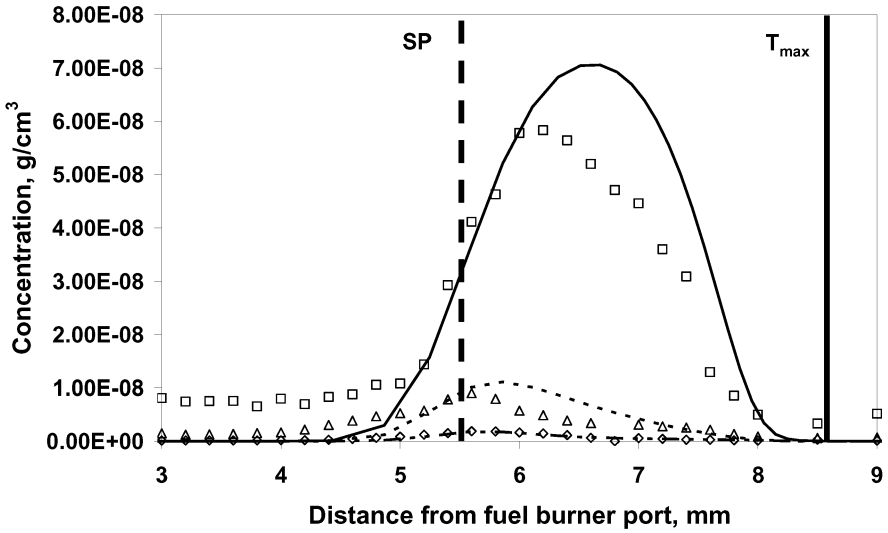

Fig. 3 Qualitative comparison between LIF and LII emissions at different wavelengths and particle classes for methane LIF@300 (□) LIF@330 (○) LIF@430 (◊) LII@550 (Δ) compared with HMM-PAH (__), particles from 1nm to 3nm (- -) particles from 3nm to 6nm (__ - - __ - -) particles larger than 6nm (__ __). Modeled stagnation plane SP (dashed vertical line) and flame front Tmax (solid vertical line) are also reported.

LIF@310 well correlates with HMM-PAHs, LIF@350 correlates with 1nm<DP<3nm particles, LIF@440 correlates with 3nm<DP<6nm particles and LII with primary soot particles.
Analysis of model results allows to better describe the mechanisms of particle formation.
Particle inception can be considered the result of a chemical growth and a physical process involving gas-phase and high-molecular mass aromatic coagulation. In the region close to the flame front where the temperature is relatively high and radicals are abundant, inception is well described by chemical growth: aromatic molecules add

aromatic radicals which lead to the formation of aromatic-aromatic linked, bi-phenyl like, structures.

These compounds behave spectroscopically as the isolated gas-phase PAHs of which they are comprised, exhibiting fluorescence in the UV at 310 nm and 350 nm.

These compounds are moved away from the flame zone towards the stagnation plane by convective, diffusive and thermophoretic fluxes crossing region of the flame characterized by the presence of acetylene and other aromatics. These latter compounds contribute to the molecular weight growth process forming particles of increasing sizes which exhibit a fluorescence more shifted in the visible at 440 nm.

Coagulation of these particles and graphitisation and thermal annealing (not modeled in the presented work) lead to the formation of solid structures which exhibit also incandescence emission.

Solid particles are transported toward the stagnation plane as shown by the decrease of incandescence, whereas high-molecular mass species responsible for visible fluorescence are continuously formed also close to the stagnation plane.

Indeed at relatively lower temperatures and still significant concentrations of PAHs, particles continue to grow mainly through a physical coagulation of PAHs (stacked cluster PAH).

Due to the lower temperature, the coagulation process is more effective than at higher temperature since particles and molecules do not have enough thermal energy to rebound once they collide, and hence they remain attached.

The formed clusters of PAHs lose the chemical identity of gas-phase aromatics (compounds fluorescing at 310 nm) and exhibit a fluorescence more similar to that of PAH excimers hence shifted more in the visible at 350 nm and 440 nm depending on their molecular size (Miller and Herdman 2007).

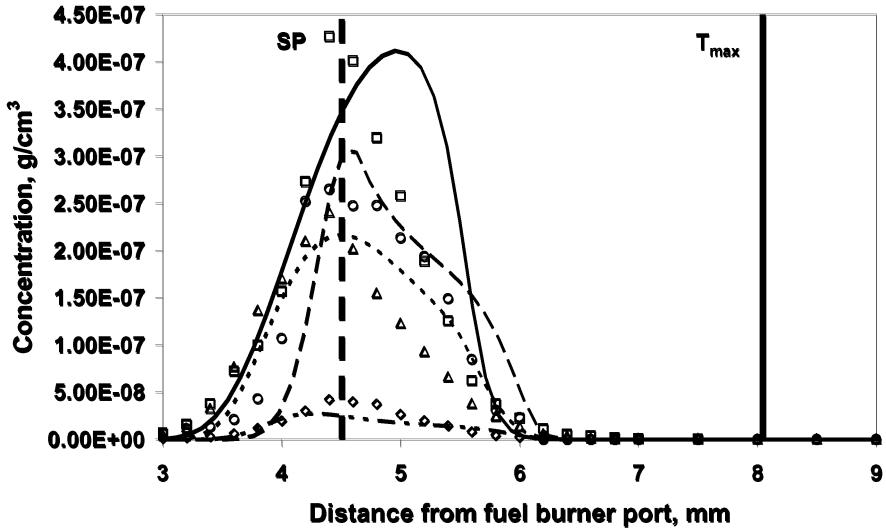

Fig. 4 *Qualitative comparison between LIF and LII emissions at different wavelengths and particle classes for ethylene LIF@300 (□) LIF@330 (○) LIF@430 (◊) LII@550 (Δ) compared with HMM-PAH (__), particles from 1nm to 3nm (- -) particles from 3nm to 6nm (__ - - __ - -) particles larger than 6nm (__ __). Modeled stagnation plane SP (dashed vertical line) and flame front Tmax (solid vertical line) are also reported.*

5. Conclusion

Methane and ethylene opposed-flow flames have been numerically and experimentally investigated. Laser induced emission spectroscopy has been used in order to detect different combustion generated species. Comparison with model predictions has been done in order to better understand the evolution of particulate in flame. The complete kinetic scheme, here used, simultaneously provides both gas-phase and particle reactions, based on sectional method. Signals at different wavelengths and different particles classes can be individuated and compared for both flames. Two different zone of formation of particulate can be distinguished for this flame configuration: close to flame front, in the oxidizer side, radical-molecule mechanism, involving C_2H_2 and PAHs, is predominant, whereas in the fuel side, due to low temperatures, coagulation of PAHs and particle are the main route to form and grow new particles.

3. References

D'Alessio A., D'Anna A., Gambi G., Minutolo P., J. Aerosol Sci. 29 (4) (1998) 397-409.

D'Anna A., Violi A., D'Alessio A., Sarofim A. F., Combust. Flame 127, 1995-2003, (2001).

D'Anna A., Violi A., Energy & Fuels, 19(1), 79-86 (2005).

D'Anna A., Kent J. H., Combust. Flame 144, 249-260, (2006).

D'Anna A., Alfe M., Apicella B., Tregrossi A., Ciajolo A., Energy & Fuels 21 (5) (2007) 2655-2662.

D'Anna A., Sirignano M., Commodo M., Pagliara R., Minutolo P., Comb. Tech., 180(5), 950-958 (2008).

Dockery D. W., Pope C. A., Xu X., Spengler J. D., Ware J. H., Fay M. E., Ferris B. G., Speizer F. E., New England Journal of Medicine 329 (1993) 1753-1759.

Hwang J. Y., Chung S. H., Combust. Flame 125:752–762 (2001).

Li Z., Wang H., Physical Rev., E70, 021205 (2004).

Miller J. H., Herdman J. D., "Computational and Experimental Evidence for Polynuclear Aromatic Hydrocarbon Aggregation in Flames" in International Workshop on Combustion Generated Fine Carbon Particles, Villa Orlandi, Italy, May 13-16, 2007.

Minutolo P., D'Anna A., D'Alessio A., Combust. Flame 152 (1) (2008) 287-292.

Oberdorster G., Sharp Z., Atudorei V., Elder A., Gelein R., Kreyling W., Cox C., J. Tox and Env. Health, Part A 65 (20) (2002) 1531-1543.

Olten N., Senkan S., Combust. Flame 118 (3) 500-507, (1999).

Sgro L. A., Basile G., Barone A. C., D'Anna A., Minutolo P., Borghese A., D'Alessio A., Chemosphere 51 (10) (2003) 1079-1090.

Vander Wal R. L., Twenty-Sixth Symp. on Comb., pp. 2269–2275 (1996).

Vander Wal R. L., Jensen K. A., Choi M. Y., Combust. Flame 109: 399-414, (1997).

Zhao B., Yang Z., Wang J., Johnston M.V., Wang H., Aerosol Sci. Technol. 37 (8) (2003) 611-620.